This document was prepared for the ETI by third parties under contract to the ETI. The ETI is making these documents and data available to the public to inform the debate on low carbon energy innovation and deployment.

Programme Area: Marine

Project: PerAWAT

Title: Scientific Report for the SpecWEC Modelling Tool - Part 1

Abstract:

This document contains the scientific report for the SpecWEC numerical modelling tool, which is part of WG1 WP2 D8. It begins by discussing the base spectral wave model TOMAWAC, which SpecWEC is based on. The governing equations of TOMAWAC are shown, and the algorithm TOMAWAC uses to solve those equations is detailed. The phase-averaging assumption made in spectral wave models is discussed, as is the theory behind the SpecWEC modelling tool. Finally, results from modelling an array of point absorbers with SpecWEC are compared to both a linear phase-resolving numerical model, and wave tank experimental data. Considering that SpecWEC is a new methodology with scope for significant improvement. these analyses indicate that SpecWEC has the potential be a useful tool for power production estimation, particularly when averaging over a large number of devices and sea states.

Context:

The Performance Assessment of Wave and Tidal Array Systems (PerAWaT) project, launched in October 2009 with £8m of ETI investment. The project delivered validated, commercial software tools capable of significantly reducing the levels of uncertainty associated with predicting the energy yield of major wave and tidal stream energy arrays. It also produced information that will help reduce commercial risk of future large scale wave and tidal array developments.

Scientific Report for the SpecWEC modelling tool

WG1 WP2 D8 – Part 1

DOCUMENT CONTROL SHEET

Client	Energy Technologies Institute
Contact	Geraldine Newton-Cross
Project Title	PerAWaT
Document N^{o}	QUB-130605
Classification	Not to be disclosed except in line with the terms of the Technology Contract
Date	17th September 2013

REV.	Issue date	Purpose of issues	Prepared by	Checked by
0.1	05/06/13	Draft for internal comment	KS	MF
1.0	19/06/13	Draft for comment by GH	KS	MF
2.0	09/07/13	Final version for release	MF	
3.0	17/09/13	Modified in response to comments from ETI	MF	

Approved for release by:

CONTENTS

Executive summary

This document contains the scientific report for the SpecWEC numerical modelling tool, which is part of WG1 WP2 D8. It begins by discussing the base spectral wave model TOMAWAC, which SpecWEC is based on. The governing equations of TOMAWAC are shown, and the algorithm TOMAWAC uses to solve those equations is detailed. Next, the phase-averaging assumption made in spectral wave models is discussed. It is argued that, although phase-dependent interactions in wave farms may be significant at single frequencies, in polychromatic waves the constructive and destructive interactions tend to cancel each other out so that phase-dependent effects are not significant. Therefore, it is considered valid to use a phase-averaged model to estimate power capture for arrays of wave energy devices. Moreover, this is particularly true when averaging over many sea states and devices, which is necessary when calculating the mean annual energy production of a wave farm.

The theory behind the SpecWEC modelling tool is discussed next. The use of a sub-grid scale representation for each wave energy device is detailed. Three different options are given for the user to represent wave energy converters: a simplified linear frequency and directional dependent representation, a more sophisticated representation of a point absorber, and a shell representation that the user can complete to represent their own device. Each representation is described in detail, including a description of all the equations solved by the subroutines.

Finally, results from modelling an array of point absorbers with SpecWEC are compared to both a linear phase-resolving numerical model, and wave tank experimental data. These results were described in detail in WG1 WP2 Deliverables 4 and 5. It is shown that the difference between total array power production calculated by SpecWEC and the linear phase-resolving numerical model is less than 9%, and the difference between total array power production calculated by SpecWEC and the wave tank data is less than 12%. Considering that SpecWEC is a new methodology with scope for significant improvement. these values indicate that SpecWEC has the potential be a useful tool for power production estimation, particularly when averaging over a large number of devices and sea states.

1 List of symbols

a	Amplitude of spectral wave component
A_C	Representation area/calibration factor of the wave energy converter source term
A	Frequency-dependent added mass coefficient
B	Frequency-dependent added damping coefficient
c_g	Wave group velocity
c_σ	Wave propagation velocity in spectral space
c_θ	Wave propagation velocity in direction
C	Frequency dependent coefficient of the wave energy converter source term
D	Directional dependent coefficient of the wave energy converter source term
E	Spectral energy density
F_c	Coulomb friction force on the wave energy converter
F_W	Incident wave force on the wave energy converter
F_{PTO}	Power-take-off force on wave energy converter
g	Gravitational acceleration
G	Frequency-dependent incident wave force coefficient
H_s	Significant wave height
I	Frequency-dependent complex response amplitude of the WEC
k	Wave number
K	Hydrostatic stiffness of wave energy converter
l	Wave energy converter separation distance
n_θ	Number of computational directions used by TOMAWAC
N	Wave action density
p	Uncertainty in the incident wave field
P_{abs}	Power absorbed by the wave energy converter
P_{rerad}	Power re-radiated by the wave energy converter
P_{abs_rad}	Power absorbed by the wave energy converter that is subsequently re-radiated
PWD	Principle wave direction of sea-state
q	Wave energy converter interaction factor
s	Directional spreading parameter of sea-state
S	Sum of all source/sinks
S_{in}	Source strength due to wind generation
S_{nl3}	Source strength due to nonlinear triad interactions
S_{nl4}	Source strength due to nonlinear quadruplet interactions
S_{wc}	Source strength due to white-capping
S_{db}	Source strength due to depth-induced wave breaking
S_{bf}	Source strength due to bottom friction

S_{WEC}	Source strength due to wave energy converter
t	Time
T	Wave period
T_e	Energy period
U	Background current
x	Cartesian spatial coordinate
X	Wave energy converter heave displacement
y	Cartesian spatial coordinate
σ	Intrinsic wave frequency
ω	Observed wave frequency
θ	Directional coordinate
θ_0	Direction of wave propagation
ν	Ratio of wave frequency to natural frequency used in simplified WEC source term
μ	Ratio of inertial and radiation forces used in simplified WEC source term
λ	Ratio of applied to radiation damping used in simplified WEC source term
η	Sea surface elevation
ε	Phase of spectral wave component
ρ	Density of water
Λ	Linear power-take-off coefficient
$\hat{v}$	Expected velocity of the wave energy converter
γ	Spectral bandwidth parameter used in JONSWAP spectrum

2 Introduction

2.1 Scope of this document

The SpecWEC (Spectral representation of a Wave Energy Converter) tool is an add-on to the TOMAWAC spectral wave model that allows for the modelling of arrays of wave energy devices. In Section 2, the spectral wave model TOMAWAC is described. This section includes the spectral wave theory, algorithms the model uses to implement that theory, and justification of assumptions that are made in the theory. Section 3 describes the modifications that were made to TOMAWAC to create the SpecWEC model. This includes description of two representations of wave energy converters: a simplified linear model, and a more realistic point absorber model, where the hydrodynamics are linear, but a non-linear PTO force (equivalent to coulomb damping) is included as a configuration option. Section 4 describes the results of verification and validation of SpecWEC and

finally Section 5 discusses the potential for further development of SpecWEC and the use of phase-averaging models for calculating WEC array interaction factors in general.

2.2 Relationship to other deliverables

This scientific report is Part 1 of WG1 WP2 D8, which also includes a User Report (Part 2) and the final release of the SpecWEC modelling tool. SpecWEC was verified and validated against other numerical models in WG1 WP2 D4 and wave tank experimental data in WG1 WP2 D5. The beta release of SpecWEC was given in WG1 WP2 D3. The representation and implementation of SpecWEC were first described in WG1 WP2 D1 and D2, respectively.

2.3 WG1 WP2 D8 Acceptance criteria

The acceptance criterion for the scientific report for WG1 WP2 D8 states that it should detail all theoretical assumptions and algorithms in sufficient detail that it can be understood and followed by a third party. The Scientific Report should also indicate the level of agreement between the numerical- and scale-model data. The algorithms and assumptions for the base model TOMAWAC are described in Section 2, and those for SpecWEC are described in Section 3. Finally, a summary of the verification and validation of SpecWEC (that was carried out for WG1 WP2 D4 and D5) is included in Section 4.

3 TOMAWAC

The TELEMAC-based Operational Model Addressing Wave Action Computation (TOMAWAC) was developed by EDF in Chatou, France. TOMAWAC was designed to represent the sea state at any given time using statistical methods, as the underlying fluid dynamics are too complicated to allow for a deterministic description of the surface wave climate over large areas within an acceptable computational time-frame. This is achieved by solving the wave action conservation equation and makes TOMAWAC a member of the family of 3rd generation spectral wave models. Wave action, denoted by $\boldsymbol{N}$, is defined as the energy density of the directional frequency spectrum divided by the intrinsic frequency ($\boldsymbol{N} = \boldsymbol{E}/\boldsymbol{\sigma}$) and is a multi-dimensional variable which is a function of horizontal space, time, direction, and frequency ($\boldsymbol{N}(\boldsymbol{x}, \boldsymbol{y}, \boldsymbol{\sigma}, \boldsymbol{\theta})$). The intrinsic frequency is defined as the $\boldsymbol{\omega} - \boldsymbol{kU}$ and $\boldsymbol{\omega}$ is the observed wave frequency, $\boldsymbol{k}$ is the wave number and $\boldsymbol{U}$ is the background current. Wave action is used in the model because it is conserved even in the presence of time-varying background currents, while spectral energy density is not, which is why spectral wave models solve the conservation of wave action equation given as (see for example pg47 in Komen *et al.* 1994):

$$\frac{\partial N}{\partial t} + \nabla_x \cdot \left[\left(\overrightarrow{c_g} + \vec{U}\right)N\right] + \frac{\partial c_\sigma N}{\partial \sigma} + \frac{\partial c_\theta N}{\partial \theta} = \frac{S}{\sigma} \qquad (2.1)$$

Here c_g is the group velocity, and $\boldsymbol{c_\sigma}$ and $\boldsymbol{c_\theta}$ are propagation velocities in spectral space where $\boldsymbol{\sigma}$ is the intrinsic wave frequency and $\boldsymbol{\theta}$ is the wave direction. Finally, $\boldsymbol{S}$ represents any source or sink term which adds, removes or transfers energy in the system.That in the presence of marine currents wave action is conserved rather than wave energy is conserved is because marine currents cause a change in wave energy. For example the energy (and frequency) of a pendulum is not conserved when its length is changed due to the necessary work done in changing the length of the pendulum. However, the energy divided by the frequency (i.e. action) is conserved and may be viewed as an "adiabatic invariant". The equivalent occurs to waves when the underlying marine current changes, so that the wave action (the "adiabatic invariant") is conserved whilst the wave energy is not. Further discussion of this can be found in pages 19-47 of Komen et. al. (1994).

3.1 Convection of wave action

The first term on the left hand side of the wave action equation (Equation 2.1) represents the change of wave action density in time. The next three terms are known as convection terms. In the absence of any source terms, the wave action density is conserved, and therefore these terms can only serve to move energy around in geographic, frequency, and directional space (that is, they cannot act as sources or sinks of wave action). The first convection term represents the horizontal propagation of energy; it can be seen that the speed that the energy moves is the sum of the group velocity and the background current. The second convection term represents the shifting of energy between frequencies, which can occur because of variations in the mean currents and the water depth. Finally, the third convection term represents the shifting of energy in directional space, typically termed refraction, again due to either variable water depth or currents.

3.2 Source terms

The aggregated source term represents the mechanisms by which energy is gained and lost. Currently, in spectral wave models the aggregated source term is typically broken down into six independent components, as follows:

$$\boldsymbol{S = S_{in} + S_{nl3} + S_{nl4} + S_{wc} + S_{db} + S_{bf}} \qquad (2.2)$$

where $\boldsymbol{S_{in}}$ represents generation of waves by the wind, $\boldsymbol{S_{nl3}}$ represents nonlinear triad interactions, $\boldsymbol{S_{nl4}}$ represents nonlinear quadruplet interactions, $\boldsymbol{S_{wc}}$ represents energy dissipation due to white capping, $\boldsymbol{S_{db}}$ represents energy dissipation due to depth-induced wave breaking, and finally $\boldsymbol{S_{bf}}$ represents energy dissipation due to bottom friction. A brief description of the source term components follows here.

Generation of waves by the wind ($\boldsymbol{S_{in}}$) occurs through two different mechanisms. Energy transfer from the wind to the waves starts with resonance with wind-induced pressure fluctuations, which leads to the growth of small waves (Phillips, 1957). This growth is linear in time. As the wave grows, it distorts the wind field, which in turn leads to faster growth of the wave. This feedback mechanism follows the resonance mechanism, and results in an exponential transfer of energy from the wind to the waves with time (Miles, 1957). The wind source term for the wave action equation takes into account both the linear and exponential growth terms. The magnitude of the source term is dependent on the wind strength and direction as well as the wave age, frequency, and direction.

Nonlinear wave-wave interactions occur when a set of waves with resonant frequencies exchange energy across the frequency spectrum. There are two types of nonlinear wave-wave interactions: triad (or three-wave) interactions ($\boldsymbol{S_{nl3}}$), which are important in shallow water, and quadruplet (or four-wave) interactions ($\boldsymbol{S_{nl4}}$), which are important at deep and intermediate water depths. Quadruplet interactions act to shift energy away from the peak spectral frequency, both to higher and lower frequencies. Triad interactions mostly tend to shift energy from lower frequencies to higher frequencies. Although it is possible to write an analytical expression for the nonlinear wave-wave interactions and solve for the wave action equation source terms, this process is computationally intensive, and therefore not commonly implemented. Instead, third generation spectral wave models use an approximation of the two interaction source terms in which the magnitude of the source term is dependent on the wave number and frequency of the existing wave action spectrum (Hasselmann et al., 1985).

Wave energy dissipation through white capping ($\boldsymbol{S_{wc}}$) occurs as a wave gains energy from the wind, steepens, and becomes unstable in a highly nonlinear process. Approximation of the magnitude of this dissipation as applied in third generation spectral wave models is dependent on the wave steepness, the wave energy, and the mean frequency and wave number (Hasselmann, 1974). Wave energy dissipation also occurs due to depth-induced wave breaking ($\boldsymbol{S_{db}}$). As waves propagate towards the shoreline the shoaling water depth results in larger wave heights, which subsequently leads to instability and wave breaking. Obviously, this process is most important in shallow water. Because experimental data have shown that depth-induced breaking does not result in changes in wave spectral shape, the magnitude of the source term is simply dependent on the wave action field (Eldeberky and Battjes, 1995). The last form of energy dissipation which can act to remove energy from surface waves is bottom friction ($\boldsymbol{S_{bf}}$). Because orbital wave motions can extend down to the ocean bottom, the resulting drag must be taken into account. In third generation spectral wave models, the bottom friction source term is typically represented with a quasi-linear drag term where the drag coefficient may be determined empirically and is typically

dependent on the expected value of absolute velocity at the seabed (Collins, 1972; Madsen et al., 1988).

It should be noted that in general, the source terms used in third generation spectral wave models are based on semi-empirical models. That is, the source terms have been parameterized based an a simplified model of the relevant physical process and then calibrated based on observations. These source terms are under continual development, which allows the accuracy of spectral wave models to continue to improve. Further information on the parameterization of these source terms can be found in Komen, et. al. (1994).

3.3 Numerical solver

TOMAWAC solves the wave action equation in two steps: first by finding an interim solution of the wave action equation with no source terms, and then applying the source terms to this interim solution. The separation of the numerical solver into two steps simplifies the solver because the propagation model does not need to consider the change in the wave action and the change in wave action does not need to consider the propagation, which allows the use of the method of characteristics. However, this means that the solution at an interim time step is required.

In the first step (called the convection step), the homogeneous equation is solved:

$$\frac{\partial N}{\partial t} + \nabla_x \cdot \left[\left(\overrightarrow{c_g} + \vec{U} \right) N \right] = 0 \qquad (2.3)$$

This equation is discretized as follows:

$$\frac{N^* - N^n}{\Delta t} = -\nabla_x \cdot \left[\left(\overrightarrow{c_g} + \vec{U} \right) N \right]^n \qquad (2.4)$$

Here, the * superscript indicates the interim time step, and the n superscript denotes the previous time step. For this first step, TOMAWAC uses the method of characteristics, which is a technique for transforming the partial differential equation (PDE) that must be solved (the homogeneous wave action equation) into a system of ordinary differential equations (ODEs). This is done by mathematically defining functions in space and time (characteristics) upon which the PDE collapses to ODEs. The full derivation of this method can be found in (Esposito, 1981). The advantage of this method is that in the absence of a background current that changes in time, the characteristics calculation only needs to be performed once, at the very beginning of the model run. During the subsequent time steps, the only operation that is performed is interpolation of the characteristics to the mesh grid, which is substantially less computationally expensive than the characteristic calculation itself.

The second step in the solver is the source term integration step. Here, the non-homogenous equation is solved:

$$\frac{\partial N}{\partial t} = \frac{S}{\sigma} \qquad (2.5)$$

This step is discretized as:

$$\frac{N^{n+1} - N^{*}}{\Delta t} = \frac{S^{n+1} + S^{*}}{2\sigma} \qquad (2.6)$$

Here, the $n+1$ superscript indicates the next time step, and the * superscript indicates the interim time step.

3.4 Phase-averaging assumption

TOMAWAC is a phase-averaging model, which means that the assumption has been made that the phases of individual waves are randomly distributed. The advantage of this simplification is the ability of the phase-averaging model to solve a much larger computational domain (containing a large number of interacting objects) in the same time as the smaller domain of a phase-resolving model. The disadvantage of the phase-averaging technique is the inability to directly account for phase-dependent processes such as diffraction. However, most third generation spectral wave models (including TOMAWAC) have a parametric phase-decoupled model of diffraction built into the solver. This parameterization of diffraction is based on the mild-slope equation, and expresses the diffraction in terms of the directional turning rate of the individual wave components (Holthuijsen et al., 2003). This representation has been shown to produce reasonable results in most situations except for regions in close vicinity to an obstacle that stops the propagation of waves, resulting in a wave shadow, *viz*. a reduction in wave height in the lee of the obstacle.

Previous hydrodynamic numerical modelling work has shown that arrays of wave energy converters are subject to an effect known as array interaction, in which the separation distance between devices can influence the power capture of the device due to phase differences in the wave field (Thomas and Evans, 1981; Fitzgerald and Thomas, 2007). This seems to indicate that a phase-averaging model, which cannot capture these effects, is not suitable for representation of arrays of wave energy converters. However, the significant array interaction obtained in these studies was derived for monochromatic waves and idealized devices, consisting of perfectly controlled wave energy converters and clearly defined incident waves. In the real ocean, there is much uncertainty associated with the wave energy converter position, the incident waves, and the wave energy converter dynamics. Here, statistical analysis is applied to a more realistic wave energy converter array and sea-state, and it is shown that the expected array interaction effects are not as significant as previously perceived. That is, although for a particular single frequency and WEC spacing the array

interaction factors may be large, they also tend to oscillate with states of large constructive interactions being balanced by states of large destructive interference. The net consequence is that these tend to cancel each other out so that although the interaction effects are influential, they are not as large as a monochromatic analysis may suggest.

First, we consider the source of the uncertainties in both the incident wave field and the wave energy converter position. Incident wave fields are often represented in a simplified manner in numerical models, such as a Bretschneider spectrum which has only two parameters for input. However, many sea states are bimodal, a situation which is clearly poorly represented with only two parameters. Also, the method of obtaining these parameters from a scatter diagram is flawed because the binning of the data causes loss of information. For measured data, an incident wave field represented with a data spectrum from a buoy or other observational platform has inherent uncertainties associated with the collection and processing of that data. Alternatively, incident wave spectra which are taken from a model such as WAM have uncertainties associated with the calibration of the model.

Now consider wave energy converter position. After wave energy converters have been deployed in an array, the actual position of each device may be slightly different than the planned position, resulting in uncertainty in the device positions. Of course the array could be surveyed after the deployment, but any pre-deployment modelling should account for positional uncertainty. Moreover, wave energy converters that are deployed with compliant moorings will have uncertainties in their position as they can move around in the water because of marine currents and low frequency oscillations on their moorings. Marine currents also effectively contribute to the positional uncertainty of wave energy converters, as a wave propagating in the same direction as a marine current will travel faster between devices, effectively shortening their separation distance. Conversely, a wave propagating against a background current will travel more slowly between devices, resulting in a larger effective separation distance.

A statistical analysis is used to evaluate the expected array interaction factor considering the above described uncertainties. Two examples of wave energy converter configurations are considered. The first is of a pair of heaving truncated cylinders with a 10.0 metre diameter and 10.0 metre draft with optimum damping, and the second of a pair of surging truncated cylinders with a 10.0 metre diameter and 10.0 metre draft with optimum damping. The individual array interaction factors (defined as each WEC's power capture in the array divided by the WEC's power capture in isolation) are calculated assuming that linear wave theory applies and the hydrodynamic coefficients have been obtained using WAMIT. For both examples it is assumed that the amplitudes of motion of the WECs are unconstrained and that the wave energy converter array is aligned with the direction

of propagation of waves, which should result in the largest array interaction factors. It can be seen that the fluctuation variation inthe array interaction factors occurs more frequently as the wave period decreases and the separation distance increases (Figures 1 and 2).

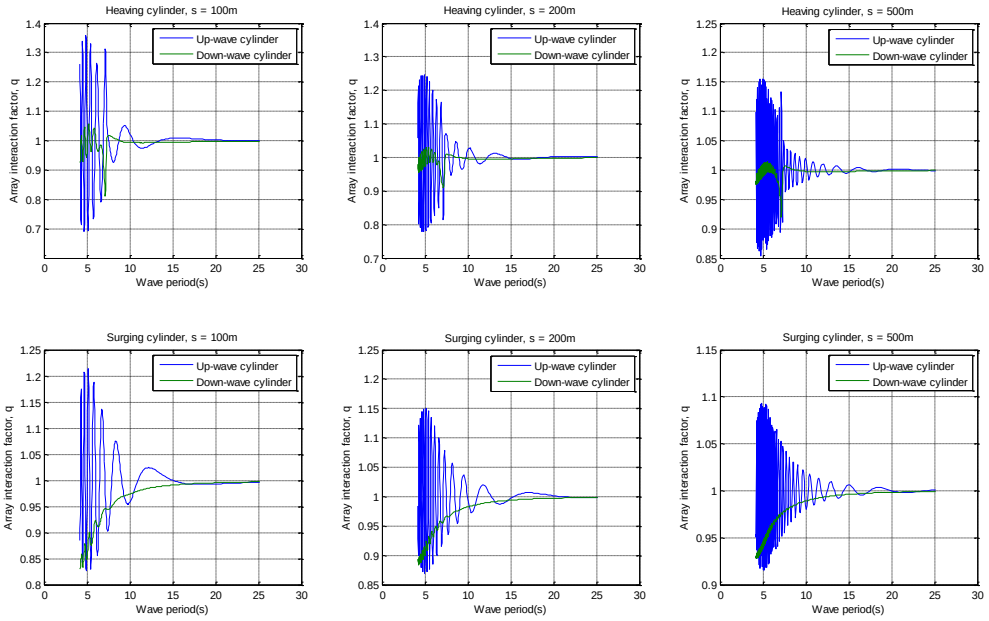

Figure 1: The variation of array interaction factors with wave period for the up-wave (blue line) and down-wave (green line) cylinders in monochromatic waves. The top panels are for the heaving buoy example, and the bottom panels are for the surging buoy example. The separation distance of the buoys increases from the left panels to the right panels.

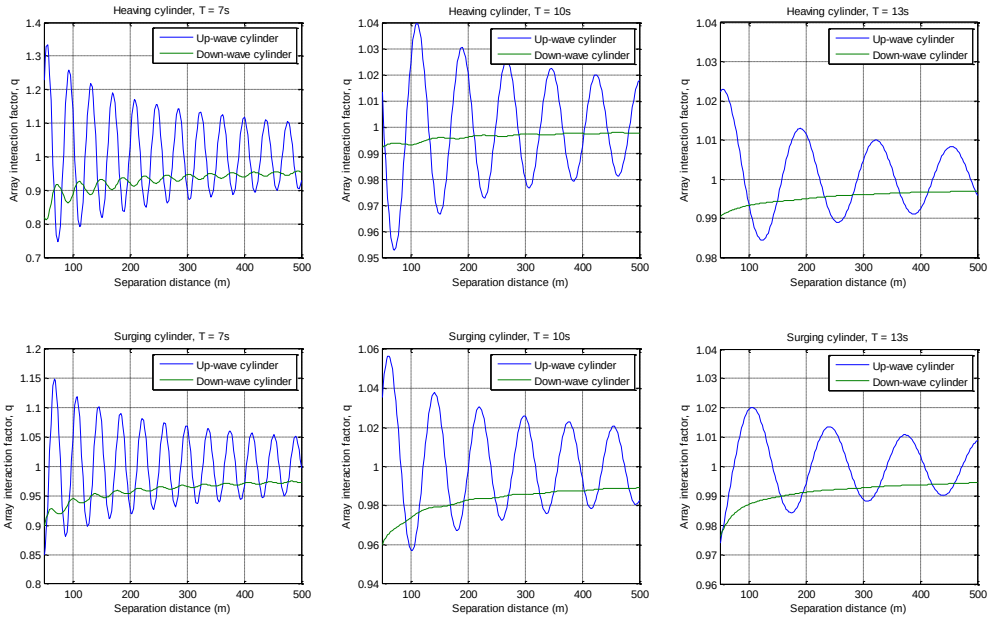

Figure 2: The variation of array interaction factors with separation distance for the up-wave (blue line) and down-wave (green line) cylinders in monochromatic waves. The top panels are for the heaving buoy example, and the bottom panels are for the surging buoy example. The wave period increases from the left panels to the right panels.

Next, the expected value of the array interaction factor is defined as follows:

$$\overline{\boldsymbol{q}(\boldsymbol{T},\boldsymbol{d})} = \int_{\boldsymbol{0}}^{\infty}\int_{\boldsymbol{0}}^{\infty} \boldsymbol{p}(\boldsymbol{T})\boldsymbol{p}(\boldsymbol{l})\boldsymbol{q}(\boldsymbol{T},\boldsymbol{l})\boldsymbol{dTdl} \qquad (\mathbf{2.7})$$

where $\overline{\boldsymbol{q}(\boldsymbol{T},\boldsymbol{d})}$ is the expected value of the array interaction factor $\boldsymbol{q}(\boldsymbol{T},\boldsymbol{l})$, $\boldsymbol{p}(\boldsymbol{T})$ is the uncertainty associated with the incident wave field (here represented as a probability density function for the wave period), and $\boldsymbol{p}(\boldsymbol{l})$ is the uncertainty associated with the wave energy converter position (again represented as a probability density function). The expected value of the array interaction factor is calculated by assuming that the wave period and separation distance have normal distributions with standard deviations of 1.5 seconds and 10 metres respectively. It can be seen that the variation in the expected array interaction value is much smaller than the array interaction values, and the fluctuations in the array interaction factor at short wave periods and long separation distances have largely vanished, Figure 3. It is important to note that this figure is for a monochromatic wave with uncertainty, the interaction factors for wave spectra are likely to show even less variation (as is shown below). The estimate for uncertainty in the wave period is based on the uncertainty of the ERA-40 wave atlas data (Uppala *et al.* 2005, ECWMF 2013), which is considered typical for a wave resource analysis. The separation distance uncertainty is an estimate based on the potential drift of a WEC on its moorings and the likely magnitude of marine currents.

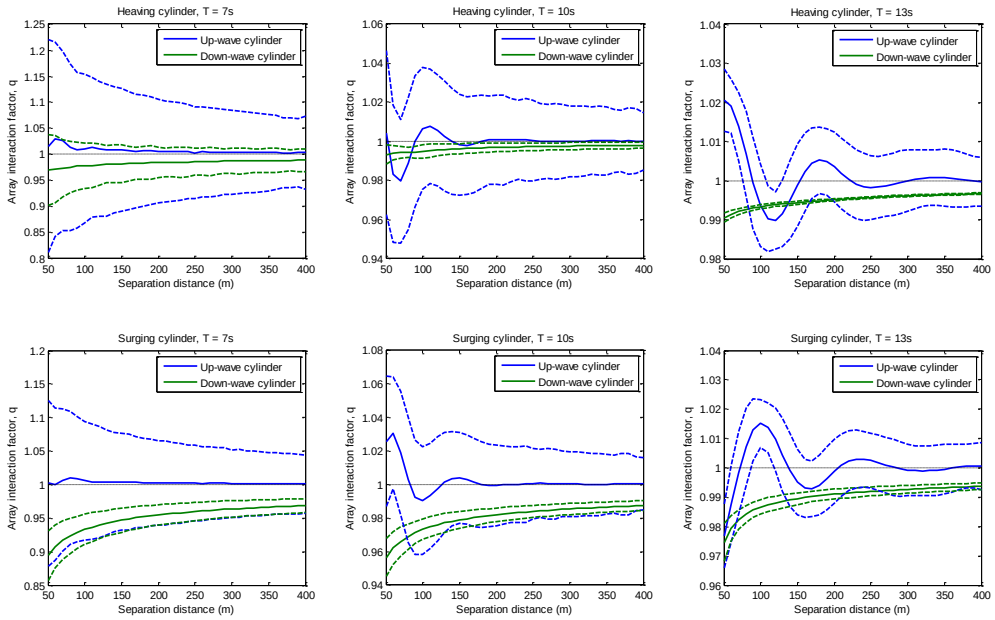

Figure 3: The variation of expected values of array interaction factor with separation distance with the dashed lines showning the 95% confidence limits for the up-wave (blue line) and down-wave (green line) cylinders for a monochromatic wave with uncertainty in the wave period and seperation distance. The top panels are for the heaving buoy example, and the bottom panels are for the surging buoy example. The wave period increases from the left panels to the right panels.

It is also possible to calculate the average array interaction for a sea state (as opposed to a single wave period), which is useful because it is a measure of how much the productivity of a single device in a wave farm may vary due to array interaction. The same wave energy configurations are applied now to a Bretschneider spectral shape with a directional spreading based on the cosine spreading function, with a parameter value, s = 15. The magnitude of the average array interaction factor is much smaller than that for a single frequency, with fluctuations in the average array interaction factor greatly reduced, and again can be seen to drop off rapidly with separation distance, Figure 4. Interestingly it can be seen that there is a clear reduction in the power capture for the down-wave WEC (seen as an interaction factor of less than 1.0), which is associated with an effective reduction in the incident wave energy. However, the up-wave WEC's interaction factor is close to 1.0[1], indicating that array interactions are not significant. Consequently, this suggests that in irregular waves the phase-dependent array interactions due to wave radiation are much less significant than interactions due to energy absorption.

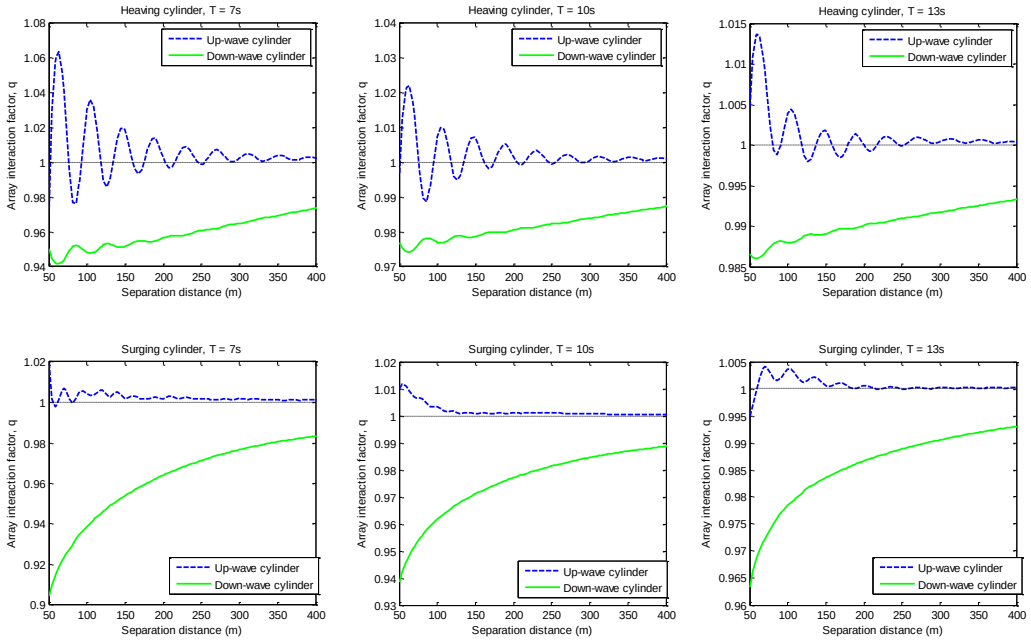

Figure 4: The variation of average array interaction factor for a Bretschneider sea state with separation distance for the up-wave (blue line) and down-wave (green line) cylinders. The top panels are for the heaving buoy example, and the bottom panels are for the surging buoy example. The spectral peak period increases from 7.0 s in the left panels to 13.0 s in the right panels.

Although the analysis has been performed for a Bretschneider spectrum, it is reasonable to assume that a similar results would be obtained for other spectra. However, it is worth noting that

[1] Close inspection of the up-wave cylinder interaction factors indicate that they are actually typically slightly greater than 1.0. This is due to the waves radiated by the down-wave cylinder increasing the energy incident on the up-wave cylinder and thus increasing the interaction factor.

any fluctuations are likely to be greater as the bandwidth of the spectrum decreases since this begins to more closely approximate a monochromatic wave.

These comparisons of array interaction factors with their expected values for two simple wave energy converter configurations suggest that array effects aren't nearly as phase-dependent as initially thought; this was achieved by consideration of a more realistic scenario. It is clear that the array interaction factor is dependent on the separation distance as it can be seen to tend towards unity as the separation distance increases. The expected values of the array interaction factors can be seen to have smaller magnitudes than the phase-dependent array interaction factors themselves. The results of these comparisons suggest that it is possible to use a phase-averaging model such as a spectral wave model to reasonably accurately capture wave energy converter array performance. Notwithstanding the apparent adequacy of a phase-averaged model, if necessary, a phase-dependent array interaction approximation could be introduced into the wave action equation in which wave energy converters which are closer than a set distance have an array interaction source/sink term which alters the wave action density at the wave energy converter location.

4 SpecWEC

SpecWEC is the augmentation of the TOMAWAC spectral wave model that allows the inclusion of individual wave energy converters. Wave energy devices are included in the TOMAWAC model by introducing an additional source term, $\boldsymbol{S_{WEC}}$:

$$\boldsymbol{S = S_{in} + S_{nl3} + S_{nl4} + S_{wc} + S_{db} + S_{bf} + S_{WEC}} \qquad (\mathbf{3.1})$$

This representation is sub-grid scale, meaning that the wave energy devices are considered to be contained within a single computational node. The representation of a wave energy converter using a single node implies that its effect on the waves can be approximated as emanating from a single point. The validity of this approximation will increase with the distance from the wave energy converter so that waves from different parts of the device cannot be distinguished. Thus, it would be expected that small devices are likely to be best approximated using a sub-grid approximation; however, larger devices typically require larger separation distances (to avoid collisions) and so the approximation may be equally valid. It is worth noting that this requirement is independent of the wavelength. It would theoretically be possible to model a large device using multiple linked source terms; however, this option is not considered in this implementation of the mode.

A sub-grid representation allows the inclusion of frequency, directional, and even sea-state dependence of each individual device in the array on the background wave field. The sub-grid representation effectively includes the effects of a wave energy converter as an additional

source/sink term in the wave action density equation. This representation can be as sophisticated or as simple as the user chooses.

Fundamentally the WEC source term defines the change in the action density due to the presence of the WEC. There are three sample source term representations provided in SpecWEC: a linear frequency/direction dependent representation, a heaving point absorber representation, and a shell subroutine for the user to develop their own representation.

4.1 Simplified linear frequency/direction dependent source term

The first representation included in the SpecWEC tool is a simple representation of a WEC in which the amount of energy removed by the WEC is dependent on both the frequency and direction of the wave:

$$\boldsymbol{S_{WEC}(\omega,\theta) = C(\omega)D(\theta)E(\omega,\theta)} \qquad \textbf{(3.2)}$$

where $\boldsymbol{S(\omega,\theta)}$ is the WEC source term strength, $\boldsymbol{E(\omega,\theta)}$ is the spectral energy density, $\boldsymbol{C(\omega)}$ is a frequency dependent coefficient, and $\boldsymbol{D(\theta)}$ is the directional dependent coefficient. For a specific wave energy converter, the frequency dependent coefficient is dependent on the specific device geometry, as well as the power take-off settings with which the device is operating. For a linear single degree of freedom system it can be shown (see Appendix B) that the percentage of maximum energy extraction, $\boldsymbol{C(\omega)}$, depends on the ratio of the frequency to natural frequency, $\boldsymbol{\nu}$, the ratio of the inertial and radiation forces, $\boldsymbol{\mu}$, and the ratio of the applied to radiation damping, $\boldsymbol{\lambda}$.

$$\boldsymbol{C(\omega) = \frac{4\lambda}{\mu^2(1/\nu - \nu)^2 + (1+\lambda)^2}} \qquad (\mathbf{3.3})$$

The user can set the values of **υ, μ,** and **λ** to match the design of their particular device. The directional dependent coefficient is simply related to the cosine squared of the wave direction: $\boldsymbol{D(\theta) = cos^2(\theta - \theta_0)}$**,** where $\boldsymbol{\theta_0}$ is the incoming wave direction. Of course in actuality the values of these variables will be frequency dependent, but this model is provided as the simplest form that may be considered as representative of a directionally-dependent WEC.

4.2 Point absorber source term

The second representation included in the SpecWEC tool is for a single degree-of-freedom WEC. This is currently the most sophisticated representation included in SpecWEC. The calculation of the source term strength begins with the determination of the frequency dependent wave component amplitude from the spectral energy density. Then, the displacement of each WEC is calculated. Two different possibilities for the power takeoff system are included in the displacement calculation: a simple linear power takeoff (defined as a producing a force that is proportional to the velocity of the WEC), and a nonlinear Coulomb friction power takeoff (defined as producing a constant force that

opposes the motion of the WEC). , From the displacement, the power absorbed and the power radiated can be calculated. A calibration is then required to convert the power values into a source term strength. These steps are described in detail in the next six subsections.

4.2.1 Calculation of wave amplitude

First, the incident wave amplitude as a function of frequency and direction must be calculated. The underlying assumption made by the TOMAWAC model is that a sea state can be represented as the linear superposition of plane progressive waves which have a random phase distribution:

$$\boldsymbol{\eta(x,t) = \sum_{j} a_j \cos\left(k_j x - \omega_j t + \varepsilon_j\right)} \quad (\mathbf{3.4})$$

Here, a_j is the amplitude of the jth wave component, k is the wavenumber, ω is the angular wave frequency, and ε is the randomly distributed phase. Using this assumption of linearity, the energy present in a particular sea state can be expressed solely in terms of the wave component amplitudes as:

$$\boldsymbol{E(\omega,\theta) = \sum_{\omega}^{\omega+\delta\omega} \sum_{\theta}^{\theta+\delta\theta} \frac{1}{2}\rho g \frac{a_j^2}{\delta\omega\delta\theta}} \quad (\mathbf{3.5})$$

Therefore, given the directional spectrum of wave energy, it is possible to determine the free surface elevation in the following manner:

$$\boldsymbol{\eta(x,t) = \int_{\omega=0}^{\infty} \int_{\theta=0}^{2\pi} \sqrt{\frac{2}{\rho g} E(\omega,\theta)} \cos(kx - \omega t + \varepsilon)\, d\omega d\theta} \quad (\mathbf{3.6})$$

The individual wave component amplitudes can be solved for as:

$$\boldsymbol{a_j = \sqrt{\frac{2}{\rho g} E(\omega,\theta)\delta\omega\delta\theta}} \quad (\mathbf{3.7})$$

In SpecWEC, the amplitude is calculated from the computational node directly upstream of the node where the WEC is located. This information from TOMAWAC can then be used to calculate the WEC's vertical displacement associated with each wave component.

4.2.2 Calculation of response

In order to solve for the motion of the WEC, several assumptions are made about the wave climate and the body motion. First, we assume that the wave steepness and the WEC body motion allow the use of a linear model. In addition, as in the TOMAWAC model, it is assumed that the sea state may be represented as the linear superposition of plane progressive waves in which the phases are randomly distributed. For the following derivation, it is assumed that the WEC is a point

absorber which only moves in the heave direction; however, it is straightforward to extend the following analysis to a device which has more than one degree of freedom.

From linearity, it follows that the WEC body displacement (in heave) $X(x,t)$ can be written in the form:

$$\boldsymbol{X(x,t) = Re\left(\sum_j I(\omega_j)\, e^{-i(\omega_j t+\varepsilon_j)}\right)} \qquad (\mathbf{3.8})$$

where I is the frequency dependent complex response amplitude of the WEC. To progress we need to derive equations to solve for this particular quantity.

The WEC body equation of motion begins with the application of Newton's second law: force equals mass times acceleration. Following the linearity assumptions described above, the forces on the WEC may be represented at any single frequency component in a linear fashion as follows:

$$\boldsymbol{F_W - A\frac{d^2X}{dt^2} - B\frac{dX}{dt} - F_{PTO} - KX = M\frac{d^2X}{dt^2}} \qquad (\mathbf{3.9})$$

where $\boldsymbol{M}$ is the mass of the body, $\boldsymbol{A}$ is an added mass coefficient representing the additional inertia due to the acceleration of the body in water, $\boldsymbol{B}$ is a damping coefficient associated with the wave energy radiated from the body, $\boldsymbol{F_{PTO}}$ is the force from the power takeoff system of the WEC, and $\boldsymbol{K}$ is the system stiffness due to hydrostatic restoring forces. Although not necessary, this model assumes that the hydrostatic stiffness coefficient is constant, which is generally considered reasonable for modelling oscillating water columns, heaving buoys and pitching flaps, $\boldsymbol{F_W}$ represents the incident wave force on the WEC body. Gathering like terms, this can be rewritten as:

$$\boldsymbol{F_W = (M+A)\frac{d^2X}{dt^2} + (B)\frac{dX}{dt} + KX + F_{PTO}} \qquad (\mathbf{3.10})$$

This equation can be written using the standard frequency domain notation as:

$$\boldsymbol{I(\omega)\left(-\omega^2\left(M + A(\omega)\right) + i\omega(B(\omega) + \Lambda) + K\right) = G(\omega)a(\omega)} \qquad (\mathbf{3.11})$$

where (3.8) has been used. The WEC body displacement is then solved for in terms of the added mass ($\boldsymbol{A}$), radiation damping ($\boldsymbol{B}$), the linearised power takeoff coefficient ($\boldsymbol{\Lambda}$) (see section 4.2.3 for further details), hydrostatic stiffness ($\boldsymbol{K}$), exciting force coefficient ($\boldsymbol{G}$), and wave amplitude ($\boldsymbol{a}$) as:

$$\boldsymbol{I(\omega) = \frac{G(\omega)}{-\omega^2\left(M + A(\omega)\right) + i\omega(B(\omega) + \Lambda) + K}a(\omega)} \qquad (\mathbf{3.12})$$

4.2.3 Power take off

There are two possibilities included in the point absorber representation for the power take off. The first is a linear power take off, and the second is a nonlinear Coulomb friction damping representation. A linear power take-off generates a force on the WEC that is proportional to velocity and would be a reasonable representation of a Wells turbine, whilst a Coulomb friction

power take-off generates a constant force that opposes the WEC's motion and would be a reasonable representation for constant pressure hydraulic cylinder. For a linear power take off, the PTO damping coefficient ($\boldsymbol{\Lambda}$) can be set by the user directly. For the Coulomb friction representation, the quasi-linear power take off coefficient is given by

$$\boldsymbol{\Lambda} = \sqrt{\frac{\boldsymbol{2}}{\boldsymbol{\pi}}} \frac{\boldsymbol{F_c}}{\widehat{\boldsymbol{v}}} \qquad (\mathbf{3.17})$$

Here, $\boldsymbol{F_c}$ is the Coulomb friction damping force, and $\widehat{\boldsymbol{v}}$ is the expected velocity, calculated as follows:

$$\widehat{\boldsymbol{v}} = \sum_{\boldsymbol{i=1}}^{\boldsymbol{i=N}} \frac{\boldsymbol{1}}{\boldsymbol{2}} \boldsymbol{\omega_i^2} |\boldsymbol{I_i}|^2 \qquad (\mathbf{3.18})$$

This representation is based on the method of statistical linearization (see for example Roberts and Spanos 1990). This requires that there is a random phase between the wave components, which is a standard assumption in ocean wave modelling and spectral wave models. Indeed similar techniques are used to represent the other source terms such as bottom friction and white-capping. Effectively this means that in solving for each wave component only the expected value of the other wave components are required.

This must be solved iteratively. The iterative process begins with the choice of an arbitrary value for the quasi-linear power take off coefficient $\boldsymbol{\Lambda}$. Then, the displacement and expected velocity are calculated. Using the expected velocity, the quasi-linear power take off coefficient $\boldsymbol{\Lambda}$ can be calculated again. This process is repeated by SpecWEC within the WEC model sub-routine until the quasi-linear power take off coefficient $\boldsymbol{\Lambda}$ calculated by the two methods differs by less than 1%.

It is possible for users to add additional options for the power take-off configuration by modifying the code. Details of how to do this are included in the User Manual.

4.2.4 Calculation of absorbed power

Following calculation of the WEC displacement, the energy absorbed by each WEC can be calculated. The energy absorbed by the power take off system is represented as follows:

$$\boldsymbol{P_{abs}(\omega)} = \frac{\boldsymbol{1}}{\boldsymbol{2}} \boldsymbol{\Lambda \omega^2 |I(\omega)|^2} \qquad (\mathbf{3.13})$$

The power absorbed is introduced as a sink of energy in the wave action conservation equation at each time step.

4.2.5 Calculation of radiated power

The power radiated as a function of frequency and direction is removed from the incoming wave spectrum at each WEC location. Because the WEC's radiation pattern is assumed to be axi-

symmetric then this power is reradiated equally in all directions. Thus, the power radiated by the WEC in each directional bin is given by

$$\boldsymbol{P_{rerad}(\omega) = \frac{\sum_\theta \frac{1}{2}\mathrm{B}(\omega)\omega^2|I(\omega)|^2}{n_\theta}} \qquad (\mathbf{3.14})$$

Here $\boldsymbol{n_\theta}$ is the number of computational directions being used by TOMAWAC.

Because the radiation process conserves energy, the power that is radiated must be removed from the incident wave, as follows.

$$\boldsymbol{P_{abs\_rad}(\omega) = \frac{1}{2}\mathrm{B}(\omega)\omega^2|I(\omega)|^2} \qquad (\mathbf{3.15})$$

For axi-symmetric wave radiation the distribution of the radiated wave power is simple; however, for more complex modes the Kochin Function could be used to determine the distribution of radiated wave power. It may be expected, based on a super-position model of the incident and radiated waves that the modelling of the radiated wave is more complex. However, it can be shown (see Appendix A) that in the phase-averaged far-field then the effect of the radiated wave is to reduce the incident wave power by the sum of the absorbed/lost power and the radiated power, together with the radiation of wave power.

4.2.6 Source term strength determination

The power absorbed, radiated, and reradiated variables derived in the previous sections have units of Watts. However, the desired quantity for the source term strength has units of Watts per metre squared because TOMAWAC solves for wave energy density, or wave energy per unit area. Therefore, in order to convert the power absorbed by the device into a source term strength to be fed into the TOMAWAC model, the representative area over which the power is absorbed must be designated. The method for converting the calculated power values into a source term strength for the TOMAWAC model involves the calculation of an equivalent area over which the power can be considered to be absorbed. In this method, the source term strength is given as follows: $\boldsymbol{S_{WEC} = -\frac{P_{abs}}{A_C} - \frac{P_{abs\_rad}}{A_C} + \frac{P_{rerad}}{A_C}}$, where $\boldsymbol{A_C}$ is the area that must be designated. This area is determined using an iterative approach. The area can be determined by applying the divergence theorem, which states:

$$\boldsymbol{\iint_A \nabla \cdot E\overrightarrow{c_g} dA = \oint E\overrightarrow{c_g} \cdot \vec{n} dl = P_{abs}} \qquad (\mathbf{3.16})$$

where $\boldsymbol{E}$ is the wave energy spectral density and $\boldsymbol{c_g}$ is the wave group speed. That is, a path integral of the wave energy flux should equal the power absorbed by the device, as long as the integration path is closed and contains the wave energy device. The user must therefore perform

this iterative process to determine the calibration factor ($\boldsymbol{A_C}$) before the model runs can be completed. Although it would be expected that the appropriate area would have a simple relationship with the grid (for example equal to the sum of 1/3rd of the area of each connecting triangle), this has not been found to be the case. This issue is currently unresolved (see Section 6)However, it has been found that if the grid is regular (consisting of triangles of the same size oriented in the same direction), then the calibration factor will be the same at each point in the grid and therefore the calibration would only need to take place for one node.

4.3 Shell subroutine

Finally, a template is included for the user to modify to include a bespoke WEC representation in the SpecWEC tool. It contains the minimum code needed for the WEC source term sub-routine; it does not have an actual WEC representation. It defines the available inputs and necessary outputs required by the WEC source term subroutine. Within these input/output constraints the code may contain whatever procedures that are required to determine the WEC performance and impact on wave action density. This may include equations to solve the hydrodynamics and/or look-up tables as appropriate; the structure of the sub-routine is flexible and may be modified by the user as required.

5 Verification and Validation of SpecWEC

As part of WG1 WP2 D4 and D5, the single degree-of-freedom representation in the SpecWEC tool was used to represent a heaving point absorber and this has been compared with other numerical models (a phase-resolving frequency-domain model using hydrodynamic coefficients from WAMIT and the non-linear potential flow model OXPOT) and wave tank experimental data. The key findings of these comparisons are reproduced here. The full description of the experimental set up can be found in those deliverables. The WEC array layouts and the sea states used for validation are described in the next two sections. Results from the comparison of SpecWEC with the frequency-domain model are presented in Section 4.3, followed in Section 4.4 by results from the comparison of SpecWEC with wave tank experimental data. Finally, in Section 4.5, conclusions are drawn from the results of the verification and validation exercise.

5.1 WEC layouts

The SpecWEC model was run for the four WEC array configurations that were used for the physical tank testing: Square, Configuration A, Configuration B, and Configuration C (Figure 5). Configuration A was designed as a standard staggered row layout, while configurations B and C were

designed using WaveFarmer to achieve maximum power capture and minimum power capture respectively. In addition, SpecWEC was run for an isolated WEC to enable the array interaction factors to be calculated.

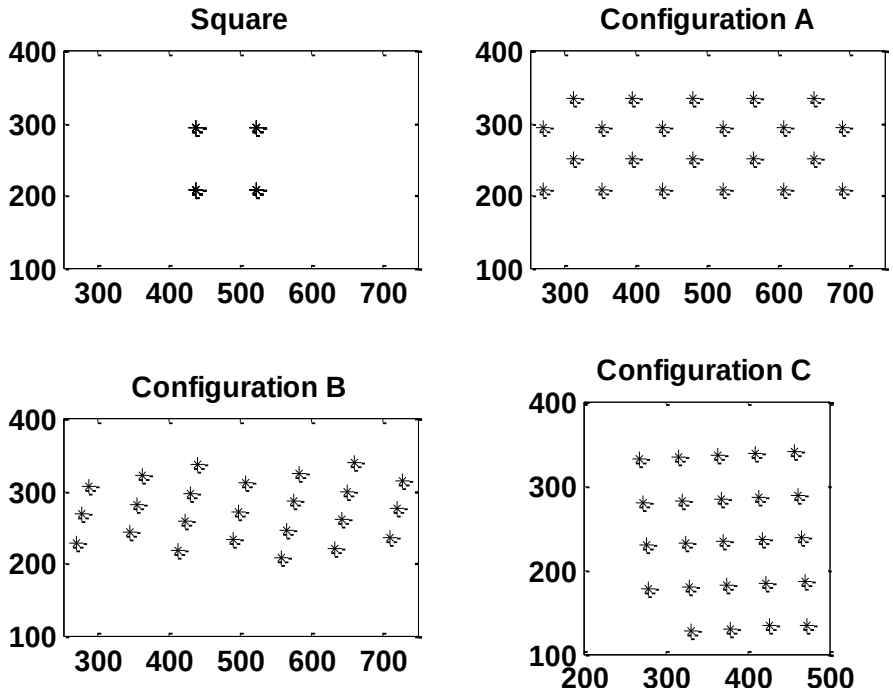

FIGURE 5: FOUR CONFIGURATIONS USED FOR THE MODEL VERIFICATION AND VALIDATION.

5.2 Sea States

Because SpecWEC is a spectral wave model, it is not capable of accurately representing monochromatic sea states and therefore only polychromatic sea states were used for comparison. The sea states used for comparison consisted of 12 polychromatic sea states with varying energy period, significant wave height, directional spreading, steepness, and mean wave direction, as shown in Table 1. In addition, because spectral wave models cannot simulate unidirectional seas directly, a sea with minimal spreading, i.e. s=45, was used as an approximation.

Sea-state	H_s	T_e	γ	s	PWD	Steepness
01	2.0	6.5	2.0	45	0	0.03
02	2.0	8.0	1.0	45	0	0.02
03	2.0	11.3	1.0	45	0	0.01
04	3.0	11.3	1.0	45	0	0.02
05	2.0	8.0	1.0	15	0	0.02
06	3.0	11.3	1.0	15	0	0.02
07	2.0	8.0	1.0	3	0	0.02
08	3.0	11.3	1.0	3	0	0.02
09	2.0	8.0	1.0	45	15	0.02
10	3.0	11.3	1.0	45	15	0.02
11	2.0	8.0	1.0	45	25	0.02
12	3.0	11.3	1.0	45	25	0.02

Table 1: sea state parameters

5.3 Results: comparison with a phase-resolving model

The SpecWEC model was compared to a phase-resolving frequency-domain model using hydrodynamic coefficients from WAMIT. The complete details of the model setup can be found in WG1 WP2 D4.

5.3.1 Isolated buoy

Comparison of the power capture of an isolated buoy for both the phase-resolving model and SpecWEC show good agreement for all twelve sea states, Table 2. Because the phase-resolving model and SpecWEC use the same equations for calculation of the WEC displacement and power absorbed, this result verifies the correct implementation of those equations in the SpecWEC model.

Sea-state	Phase-resolving model power capture (kW)	SpecWEC power capture (kW)
01	10.5	10.6
02	29.4	29.5
03	71.1	71.3
04	160.1	160.5
05	29.4	29.5
06	160.1	160.5
07	29.4	29.4
08	160.1	160.1
09	29.4	29.5
10	160.1	160.5
11	29.4	29.5
12	160.1	160.5

Table 2: Isolated buoy power capture for the phase-resolving model and SpecWEC

5.3.2 Array

	Square			Configuration A			Configuration B			Configuration C		
	WAMIT	SpecWEC	Error	WAMIT	SpecWEC	Error	WAMIT	SpecWEC	Error	WAMIT	SpecWEC	Error
SS1	41	41	+0%	217	224	+3%	219	231	+6%	261	221	-15%
SS2	118	111	-6%	605	610	+1%	720	606	-16%	650	568	-13%
SS3	282	266	-6%	1572	1456	-7%	1811	1415	-22%	1640	1315	-20%
SS4	634	598	-6%	3537	3276	-7%	4075	3184	-22%	3690	2958	-20%
SS5	116	113	-2%	606	611	+1%	707	626	-11%	644	567	-12%
SS6	630	610	-3%	3516	3282	-7%	4024	3314	-18%	3686	2946	-20%
SS7	114	114	+0%	577	591	+2%	660	624	-5%	622	568	-9%
SS8	626	617	-2%	3330	3147	-5%	3724	3302	-11%	3581	2953	-18%
SS9	116	113	-2%	606	614	+1%	694	617	-11%	639	589	-8%
SS10	630	611	-3%	3519	3302	-6%	4007	3254	-19%	3665	3092	-16%
SS11	113	115	+2%	610	613	+0%	679	643	-5%	629	589	-6%
SS12	625	624	-0%	3492	3294	-6%	3922	3423	-13%	3649	3090	-15%

Table 3: Array power capture and % error for 4 different configurations and 12 different sea states.

The total array power captures calculated by the phase-resolving model and SpecWEC show agreement with less than 10% error for the square and Configuration A layouts, and agreement with less than 23% error for the Configuration B and Configuration C layouts. There is the best agreement in all layouts in Sea States 7 and 11, which have the smaller significant wave height and an energy period of 8 seconds. Sea states 5 and 9, which have the same significant wave height and energy period, also show better agreement than the sea states with larger significant wave height and energy period. There is an overall tendency for the SpecWEC total power capture to be smaller than the phase-resolving model's total power capture, particularly in Configurations B and C.

Although WAMIT and SpecWEC both use the same dynamic model and the same hydrodynamic coefficients for an isolated buoy the average power capture for the WAMIT model will have some errors that are uncorrelated with SpecWEC. These errors are associated with the discretisation of the wave spectrum, which means that the sum of discrete frequencies will be used to estimate the average interaction factors. It can be seen from Figure 1 in Section 3.4 that the interaction factor fluctuates significantly with relatively small changes in the wave period. Thus, depending on the particular set of discrete frequencies used the average power capture could be over or under estimated, with the error decreasing as the number of wave components increased.

Comparing the magnitude of errors between the configuration it can be seen that they are significantly higher in Configurations B and C, than in the square array and Configuration A. A possible reason for this is that Configurations B and C were defined using the WAMIT model to maximize the interaction factors. It is possible that this layout optimization could have resulted in Configurations that were particularly affected by the particular frequencies used for the optimization in the discretization and thus not representative of the underlying spectrum; however, further analysis would be required to assess whether this is the actual reason for the differences between the model results.

Finally, it should be noted that the current implementation of SpecWEC does not include the effect of diffraction by the buoys. This could have the effect of under-estimating the power capture estimation from SpecWEC because the incident waves pass more easily through the array rather than being diffracted by the buoys in the array and thus creating an area of enhanced wave energy in the array. Recent research has indicated that the diffraction for WECs can be included in phase-averaged models such as SpecWEC (Babarit, Folley et. al. 2013) , but the research is still at an early stage and a representation suitable for the buoys used in this validation does not currently exist.

5.4 Comparison with wave tank experimental data

The SpecWEC model was also compared with wave tank experimental data collected from tests performed in the Portaferry wave tank as part of WG2 WP2. The complete details of this comparison can be found in WG1 WP2 D5. The key findings of the results are presented below.

5.4.1 Isolated buoy

The results for the isolated buoy comparison between SpecWEC and the wave tank power capture differ by less than 16%, as shown in Table 4.However, it should be noted that the external damping term used in the SpecWEC model was calibrated using the isolated buoy data and so therefore it is not surprising that the model is relatively accurate for a single WEC.

Sea-state	Wave tank power capture (kW)	SpecWEC power capture (kW)
01	20.4	23.5
02	63.3	58.1
03	59.3	59.1
04	106.8	97.1
05	58.0	58.1
06	95.0	97.1
07	61.3	57.9
08	101.9	96.9
09	50.6	58.1
10	89.3	97.1
11	69.3	58.1
12	103.0	97.1

Table 4: Isolated buoy power capture in kW for SpecWEC and the wave tank experiments

5.4.2 Array

	Square			Configuration A			Configuration B			Configuration C		
	Tank	SpecWEC	Error	Tank	SpecWEC	Error	Tank	SpecWEC	Error	Tank	SpecWEC	Error
SS1	94	85	-9%	287	460	+60%	333	428	+28%	338	405	+20%
SS2	223	214	-4%	1050	1186	+13%	1394	1112	-20%	874	1083	+24%
SS3	221	223	+1%	1177	1213	+3%	1383	1193	-14%	1097	1165	+6%
SS4	376	369	-2%	1999	2028	+1%	2421	2016	-17%	1810	1988	+10%
SS5	217	219	+1%	1013	1181	+17%	1276	1166	-9%	924	1060	+15%
SS6	375	374	-0%	1777	2021	+14%	2142	2073	-3%	1741	1958	+13%
SS7	210	221	+5%	1051	1105	+5%	1306	1144	-12%	970	1038	+7%
SS8	391	376	-4%	1860	1930	+4%	2251	2043	-9%	1852	1925	+4%
SS9	202	220	+8%	926	1196	+29%	1130	1153	+2%	851	1145	+35%
SS10	348	375	+8%	1762	2038	+16%	2089	2059	-1%	1751	2059	+18%
SS11	229	225	-2%	1054	1194	+13%	1371	1230	-10%	969	1145	+18%
SS12	358	381	+6%	1757	2034	+16%	2204	2144	-3%	1846	2057	+11%

Table 5: Array power capture and % error for 4 different configurations and 12 different sea states.

The total array power capture comparison between the wave tank experiments and SpecWEC shows differences of less than 10% in the square configuration, with differences of less than 28% and 34% in configurations B and C respectively. The large differences in the first sea state, which has small waves and not near the resonant period, were expected. This is because at times the buoy motion would stall and the current spectral-domain model for Coulomb friction assumes constant motion and thus does not correctly model stall, which results in larger errors in this sea state. It is possible that an improved quasi-linearisation of the coulomb friction force would be able to include the representation of stall; however, the current implementation in SpecWEC does not have this capability.

In addition, the apparent errors in SpecWEC for the Configurations A, B and C are relatively large. However, wave-tank experiments used to determine array interactions are also prone to errors that recent research indicates can be significant (Lamont-Kane, Folley and Whittaker, 2013). It is reasonable to assume that some of this error can be attributed to the wave-tank testing, although further research would be required to determine to what extent this contributes to the differences in the results shown.

5.5 Conclusions of SpecWEC verification and validation

The purpose of this comparison of the SpecWEC model to both other numerical models and wave tank experimental data was to determine the suitability of the SpecWEC model for use in power capture estimations for large WEC arrays. Because the SpecWEC model is based on a spectral wave model that is phase-averaged, it is incapable of representing close WEC array interactions that are phase-dependent. Therefore, it is not expected that the SpecWEC model can exactly reproduce the power capture of individual buoys in an array. However, it is hoped that the model will be able to provide useful information to the user about the total power production of an array. Averaging over all sea states and configurations, the difference between total array power production

calculated by SpecWEC and the phase-resolving model is less than 9%, and the difference between total array power production calculated by SpecWEC and the wave tank data is less than 12%. These values indicate that SpecWEC has the potential to be a useful tool for power production estimation, particularly when averaging over a large number of devices and sea states considering that the results are for a new technique, which can only be expected to improve with refinements.

6 Potential future development of SpecWEC

There are several steps that could be taken to improve upon the SpecWEC modelling tool. These include improving the wave energy converter representation, as well as the implementation of that representation, which currently requires a calibration factor that is dependent on the local computational mesh geometry. In addition, the alternative of using SWAN, which as another open-source spectral wave modelling tool [SWAN 2013], as the base spectral wave model should be considered.

In common with some traditional wave energy converter array models, the current SpecWEC implementation considers the waves radiated by the WEC and ignores the waves diffracted by the WEC, which is typically considered to be small. This is a reasonable approximation in many cases; however, as the WEC becomes larger relative to the incident waves diffraction by the WEC becomes more important. Consequently, it is expected that the accuracy of the WEC representation could be improved by the inclusion of the effects of diffraction by the WEC. Ongoing research at QUB indicates that waves diffracted by the WEC can be combined with the radiated waves using Kochin Functions. Furthermore, the research indicates that these can be included in phase-averaging models as detailed in Appendix A.

A current inadequacy of the SpecWEC tool is that a calibration factor must be determined iteratively to convert the power absorbed and radiated values into source term strengths for the wave action conservation equation. This calibration factor is seemingly dependent on the computational mesh in a complicated manner related to the method of characteristics that SpecWEC uses for solving the wave action equation. It is accurate but time consuming to use an iterative process to calculate the calibration factor. Investigations have revealed that if a regular grid is used (that is, one where all the triangles are the same), then the calibration factor is the same for each point, greatly reducing the time needed for calibration. The TOMAWAC development team at EDF has been consulted regarding the direct calculation of the calibration factor, but to date (July 2013) no solution has been identified. However, although an appropriate calculation factor has not yet been identified, this will continue to be investigated under the auspices of the SuperGen Centre for

Marine Energy Research (although significant progress may depend on obtaining a suitable source of further funding or resource).

Although the fundamental representation of a WEC would be the same as TOMAWAC, a future development of SpecWEC could be to implement it using SWAN as the base spectral wave model. SWAN uses a finite difference method to propagate the action density, whilst TOMAWAC uses the method of characteristics. As discussed in WG1 WP2 D2 there appears to be no fundamental reason to select one method over another; however, it is possible that direct calculation of the calibration factor is relatively simple in a finite difference method, which could make the method more attractive.

Finally, it is expected that further development in SpecWEC would include production of representations for a larger range of WECs, including validation and estimation of uncertainty. It would be misleading to give the impression that the scientific development of using phase-averaging models to determine WEC array interactions is complete. In particular, whilst the current validation gives an indication of the accuracy of SpecWEC it is not possible to distinguish between fundamental limitations of a phase-averaging model and the implementation in TOMAWAC. This is an additional area that requires further research, which will provide a benchmark against which SpecWEC can be fairly judged.

7 References

Babarit, A., Folley, M., Charrayre, F., Peyrard, C. and Benoit, M. [2013] On the modelling of WECs in wave models using far field coefficients. 10th European Wave and Tidal Energy Conference, Aalborg, Denmark

Collins, J.I. [1972] Prediction of shallow water spectra, J. Geophys. Res., 77, No. 15, pp.2693-2707

Eldeberky, Y. and Battjes, J.A. [1996]: Spectral modelling of wave breaking: Application to Boussinesq equations, J. Geophys. Res., 101, No. C1, pp. 1253-1264

ECMWF [2013] ERA-40 website, http://www.ecmwf.int/research/era/do/get/era-40, accessed 9th July 2013

Esposito, P. [1981] “Résolution bidimensionnelle des équations de transport par la méthode des caractéristiques”. Note EDF-DER-LNH HE-41/81.16.

Fitzgerald, C. and Thomas, G.[2007] A preliminary study on the optimal formation of an array of wave power devices. In: Proceedings of 7th European Wave and Tidal Energy Conference, Porto, Portugal

Hasselman, K [1974]. “On the spectral dissipation of ocean waves due to white capping”, *Boundary Layer Meteorology*, Vol. 6, pp 107-127.

Hasselmann, S., Hasselmann, K., Allender, J.H. and Barnett, T.P., 1985: Computations and parameterizations of the nonlinear energy transfer in a gravity wave spectrum. Part II: Parameterizations of the nonlinear transfer for application in wave models, J. Phys. Oceanogr., Vol. 15,pp. 1378-1391

Holthuijsen, L.H., Herman, A. and Booij, N. [2003] Phase-decoupled refraction/diffraction for spectral wave models, Coastal Engineering, Vol. 49, pp. 291-305

Komen, G. J., Cavaleri, L., Donelan, M., Hasselmann, K., Hasselmann, S. and Janssen, P. A. E. M. [1994] Dynamics and Modelling of Ocean Waves. Cambridge, Cambridge Univ. Press.

Lamont-Kane, P., Folley, M. and Whittaker, T. [2013] Investigating uncertainties in physical testing of wave energy converter arrays. 10th European Wave and Tidal Energy Conference, Aalborg, Denmark.

Madsen, O.S., Poon Y.-K., and Graber H.C. [1988] Spectral wave attenuation by bottom friction: Theory, Proc. 21th Int. Conf. Coastal Engineering, ASCE, 492-504

Miles, J.W. [1957] On the generation of surface waves by shear flows. J. Fluid Mech., Vol. 3, pp. 185-204

Phillips, O.M. [1957] On the generation of waves by turbulent wind. J. Fluid Mech., Vol. 2, pp. 417-445

Roberts, J.B. and Spanos, P.D. [1990] Random Vibrations and Statistical Linearisation, Dover Publications, New York, USA

SWAN [2013] SWAN Home page, http://swanmodel.sourceforge.net/

Thomas G. and Evans D. V. [1981] Arrays of three-dimensional wave-energy absorbers. Journal of Fluid Mechanics 108:67-88

Uppala, S.M., Kållberg, P.W., Simmons, A.J., Andrae, U., da Costa Bechtold, V., Fiorino, M., Gibson, J.K., Haseler, J., Hernandez, A., Kelly, G.A., Li, X., Onogi, K., Saarinen, S., Sokka, N., Allan, R.P., Andersson, E., Arpe, K., Balmaseda, M.A., Beljaars, A.C.M., van de Berg, L., Bidlot, J., Bormann, N., Caires, S., Chevallier, F., Dethof, A., Dragosavac, M., Fisher, M., Fuentes, M., Hagemann, S., Hólm, E., Hoskins, B.J., Isaksen, L., Janssen, P.A.E.M., Jenne, R., McNally, A.P., Mahfouf, J.-F., Morcrette, J.-J., Rayner, N.A., Saunders, R.W., Simon, P., Sterl, A., Trenberth, K.E., Untch, A., Vasiljevic, D., Viterbo, P., and Woollen, J. [2005] The ERA-40 re-analysis. Quart. J. R. Meteorol. Soc., 131, 2961-3012.doi:10.1256/qj.04.176

Appendix A: Interaction between a WEC and the incident wave

It has been noted that Kochin functions may provide a method by which array interactions can be modelled efficiently. Kochin functions can be used to represent both the diffracted and radiated wave fields. For these to be used with a spectral wave model it is necessary that a phase-averaged representation exists. Here, expressions for far-field approximations of the radiated and diffracted waves are derived, which can then be related to the appropriate Kochin function. It is shown that in the far-field approximation, the change in the wave energy due to the presence of a WEC can be decomposed into the sum of a radiation and a power absorption term.

The analysis below essentially combines the incident and radiated/diffracted wave travelling at an angle ϑ. This is used to calculate expressions for the energy flux, which is decomposed into energy flux associated with the incident wave, the radiated/diffracted wave and the interaction between these two waves. The energy flux associated with the incident and radiated/diffracted waves is non-oscillatory and easy to calculate; however, the energy flux oscillates due to the interactions as the waves go in and out of phase.

This interaction term is analysed further and using the Reimann-Lebesgue Lemma and the Method of Stationary Phase it is possible to generate an expression for this component in the far-field. It is shown that in the far-field the only persistent effect is a change in the energy flux in the direction of incident wave propagation.

Finally the derived expressions for energy flux are used to calculate the maximum power capture of a monopole wave energy converter. It is found that calculation produces the correct result as has been derived elsewhere.

A.1 Derivation

First define the pressure and velocity in the incident plane waves. The hydrodynamic pressure due to a plane wave of amplitude η_i is

$$p_i(r,\theta,z,t) = \mathcal{R}\left(\rho g \Upsilon(t)\varphi(z)e^{ikr\cos\hat{\theta}}\right)$$

Where

$$\Upsilon(t) = \eta_i e^{-i\omega t}$$

$$\varphi_i(z) = \frac{\cosh(kz)}{\cosh(kh)}$$

$$\hat{\theta} = \theta - \beta$$

The corresponding velocity potential is

$$\phi_i(r,\theta,z,t) = \mathcal{R}\left(-\frac{ig}{\omega}\Upsilon(t)\varphi(z)e^{ikr\cos\hat{\theta}}\right)$$

The wave-induced fluid velocity in the radial direction due to a plane wave of amplitude η_i is

$$u_{ir} = \frac{\partial \phi_i}{\partial r} = \mathcal{R}\left(\frac{gk}{\omega}\Upsilon(t)\cos\hat{\theta}\,\varphi(z)e^{ikr\cos\hat{\theta}}\right)$$

A.2 Radiated/diffracted wave in θ-direction

Dynamic pressure at distance *r* from source, assuming energy conservation and the Kochin function is due to scattering and radiation by the body proportional to the incident wave.

$$p_r = \mathcal{R}\left(\rho g\Upsilon(t)\varphi(z)\sqrt{\frac{2}{\pi}}\frac{H(\theta)}{\sqrt{kr}}e^{i\left(kr-\frac{\pi}{4}\right)}\right)$$

The corresponding velocity potential is

$$\phi_r = \mathcal{R}\left(-\frac{ig}{\omega}\Upsilon(t)\varphi(z)\sqrt{\frac{2}{\pi}}\frac{H(\theta)}{\sqrt{kr}}e^{i\left(kr-\frac{\pi}{4}\right)}\right)$$

The flow velocity in the radial direction is

$$u_{rr} = \frac{\partial \phi_r}{\partial r} = \mathcal{R}\left(\frac{gk}{\omega}\left(1+\frac{i}{2kr}\right)\Upsilon(t)\varphi(z)\sqrt{\frac{2}{\pi}}\frac{H(\theta)}{\sqrt{kr}}e^{i\left(kr-\frac{\pi}{4}\right)}\right)$$

A.3 Energy flux

The instantaneous radial wave energy flux is given by

$$\overline{J_r}(r,\theta,z,t) = (p_i+p_r)(u_{ir}+u_{rr}) = \frac{k\rho g^2}{\omega}\mathcal{R}\big(\mathrm{P}\varphi(z)\Upsilon(t)\big)\mathcal{R}\big(\mathrm{U}\varphi(z)\Upsilon(t)\big)$$

The average radial wave energy flux is given by

$$\overline{J_r}(r,\theta,z) = \frac{k\rho g^2}{4\omega}\varphi^2(z)\frac{1}{T}\int_t^{t+T}\big(\mathrm{P}\Upsilon(t)+\mathrm{P}^*\Upsilon^*(t)\big)\big(\mathrm{U}\Upsilon(t)+\mathrm{U}^*\Upsilon^*(t)\big)dt$$

$$\overline{J_r}(r,\theta,z) = \frac{k\rho g^2\eta_i^2}{4\omega}\varphi^2(z)(\mathrm{PU}^*+\mathrm{P}^*\mathrm{U})$$

Integrating w.r.t *z* gives

$$\overline{J_r}(r,\theta) = \frac{\rho g^2\eta_i^2}{8\omega}\tanh(kh)\left(\frac{2\mathrm{kh}}{\sinh(2kh)}+1\right)(\mathrm{PU}^*+\mathrm{P}^*\mathrm{U}) = \frac{J_i}{2}(\mathrm{PU}^*+\mathrm{P}^*\mathrm{U})$$

$$\overline{J_r}(r,\theta) = \frac{J_i}{2}\left(\left(e^{ikr\cos\hat{\theta}}+\sqrt{\frac{2}{\pi}}\frac{H(\theta)}{\sqrt{kr}}e^{i\left(kr-\frac{\pi}{4}\right)}\right)\left(\cos\hat{\theta}\,e^{-ikr\cos\hat{\theta}}+\left(1-\frac{i}{2kr}\right)\sqrt{\frac{2}{\pi}}\frac{H^*(\theta)}{\sqrt{kr}}e^{-i\left(kr-\frac{\pi}{4}\right)}\right)\right.$$
$$\left.+\left(e^{-ikr\cos\hat{\theta}}+\sqrt{\frac{2}{\pi}}\frac{H^*(\theta)}{\sqrt{kr}}e^{-i\left(kr-\frac{\pi}{4}\right)}\right)\left(\cos\hat{\theta}\,e^{ikr\cos\hat{\theta}}+\left(1+\frac{i}{2kr}\right)\sqrt{\frac{2}{\pi}}\frac{H(\theta)}{\sqrt{kr}}e^{i\left(kr-\frac{\pi}{4}\right)}\right)\right)$$

Ignoring higher-order terms in r great than $1/r$, this simplifies to

$$\overline{J_r}(r,\theta) = J_i\left(\cos\hat{\theta} + \frac{2}{\pi}\frac{|H(\theta)|^2}{kr} + \mathcal{R}\left((1+\cos\hat{\theta})e^{ikr(1-\cos\hat{\theta})-\frac{\pi}{4}}\sqrt{\frac{2}{\pi}}\frac{H(\theta)}{\sqrt{kr}}\right)\right)$$

The third term is an oscillatory function, with the frequency of oscillation increasing with the distance from the origin. Consequently, the Reimann-Lebesgue Lemma can be used to show that the asymptotic value in the far-field of the third term is zero except at locations of stationary phase. For this function the only location of stationary phase occur at θ = 0°. This term is associated with the reduction in the total incident wave energy flux, which can be calculated by integrating around the location of stationary phase. To do this it is convenient to use a complex exponential representation so that

$$\lim_{r\to\infty}\overline{\Im(0)}_{interaction} = \lim_{r\to\infty} J_i\int_{-\epsilon}^{+\epsilon}(1+\cos\hat{\theta})\mathrm{Exp}\left[i\left(kr(1-\cos\hat{\theta})-\frac{\pi}{4}\right)\right]\sqrt{\frac{2}{\pi}}\frac{H(\theta)}{\sqrt{kr}}rd\theta$$

Where $\pm\epsilon$ are infinitesimally small values. Using a Taylor series to approximate cosθ close to θ = 0° this can be written as

$$\lim_{r\to\infty}\overline{\Im(0)}_{interaction} = \lim_{r\to\infty}\frac{J_i}{k}\int_{-\epsilon}^{+\epsilon}2\cdot\mathrm{Exp}\left[i\left(kr\frac{\hat{\theta}^2}{2}-\frac{\pi}{4}\right)\right]\sqrt{\frac{2}{\pi}}H(\hat{\theta})\sqrt{kr}d\theta$$

We now use a new integration variable, which has $\pm\infty$ as integration limits[2]

$$\alpha = \sqrt{kr}\hat{\theta}$$

So that

$$\lim_{r\to\infty}\overline{\Im(0)}_{interaction} = \lim_{r\to\infty}\frac{J_i}{k}\int_{-\infty}^{+\infty}2\cdot\mathrm{Exp}\left[i\left(\frac{\alpha^2}{2}-\frac{\pi}{4}\right)\right]\sqrt{\frac{2}{\pi}}H(\hat{\theta})d\alpha$$

This has the known solution

$$\lim_{r\to\infty}\overline{\Im(0)}_{interaction} = J_i\frac{4}{k}H(\hat{\theta})$$

Replacing this back into the equation for the energy flux gives

$$\overline{J_r}(r,\theta) = J_i\left(\cos\hat{\theta} + \frac{2}{\pi}\frac{|H(\theta)|^2}{kr} + \frac{4}{k}\Re\left(H(\hat{\theta})\right)\delta(\hat{\theta})\right)$$

Where δ is the dirac delta function, which is equal to zero except when $\hat{\theta} = 0$, where the integral w.r.t θ is equal to 1.

These three terms represent the incident wave, the reduction in the incident wave due to interactions with the wave energy converter and the waves radiated by the wave energy converter.

[2] This essentially follows the procedure used by Falnes (2002) Ocean Waves and Oscillating Systems, Cambridge University Press

Therefore, in the far-field approximation, the change in energy flux due to the presence of a WEC can be represented by the sum of a power absorption term and a power radiation term.

Appendix B: Derivation of the simplified WEC model

For a WEC with a single degree of freedom the standard equation of motion in the frequency domain is given by

$$X = \frac{F_w}{[(K - M\omega^2) + j\omega(B + \Lambda)]} \tag{1}$$

Where

X is the complex amplitude of the WEC displacement

F_w is the complex amplitude of the wave force

K is the hydrostatic stiffness

M is the total mass (including added mass)

ω is the wave frequency

B is the radiation damping coefficient

Λ is the applied (PTO) damping coefficient

and the WEC's power capture is given by

$$P = \frac{\omega^2}{2}\Lambda|X|^2 \tag{2}$$

It is well known that the maximum power capture occurs when the WEC is resonant ($K = M\omega^2$) and the applied damping equals the radiation damping ($B = \Lambda$). So that the maximum power capture is given by

$$P_{max} = \frac{|F_w|^2}{8B} \tag{3}$$

So that the proportion of maximum power capture is given by

$$\frac{P}{P_{max}} = \frac{\frac{\omega^2}{2}\Lambda\frac{|F_w|^2}{(k - M\omega^2)^2 + \omega^2(B + \Lambda)^2}}{\frac{|F_w|^2}{8B}} = \frac{\omega^2\Lambda \cdot 4\mathrm{B}}{(k - M\omega^2)^2 + \omega^2(B + \Lambda)^2} \tag{4}$$

The dynamics can be non-dimensionalised using the following parameters

$$\lambda = \frac{\Lambda}{B}, \qquad \nu = \frac{\omega}{\omega_n} = \frac{\omega}{\sqrt{k/M}}, \qquad \mu = \frac{M\omega_n}{B}$$

Substituting these into Equation (4) gives

$$\frac{P}{P_{max}} = \frac{\omega^2\Lambda \cdot 4\mathrm{B}}{M^2\omega^2\omega_n^2\left(\frac{\omega_n}{\omega} - \frac{\omega}{\omega_n}\right)^2 + \omega^2B^2\left(1 + \frac{\Lambda}{\mathrm{B}}\right)^2} = \frac{4\lambda}{\mu^2\left(1/\nu - \nu\right)^2 + (1 + \lambda)^2} \tag{5}$$